

# Hybrid Analytical-Numerical Analysis of Plasmonic Photoconductive Antennas

Mohammadreza Khorshidi and Gholamreza Dadashzadeh

Department of Electrical and Electronic Engineering  
Shahed University, Tehran, 3319118651, Iran  
m.khorshidi@shahed.ac.ir, gdadashzadeh@shahed.ac.ir

**Abstract** — Photoconductive antennas (PCAs) have extensive technological applications as terahertz sources. Analysis of the performance of these antennas is typically challenging and time-consuming due to complicated interacting photonic and electromagnetic effects in the semiconductor material. The complexity even further increases in plasmonic PCAs because of the existence of periodic structures. In this paper, a numerical-analytical hybrid model is proposed for analysis plasmonic PCAs. Time-dependence and spatial-dependence of the electric field as well as carriers density generated in the semiconductor of plasmonic PCA, are calculated analytically and with finite element method, respectively. The presented model ultimately computes the current generated in the electrodes of plasmonic PCAs. Using this model, the performance of a typical plasmonic PCA as an example is investigated, and model results are validated by measurement results currently existing in the literature; though the model can also be used in the performance analysis of plasmonic PCAs with more complex periodic structures.

**Index Terms**— Finite element method, optical wave, photo-generated current, plasmonic photoconductive antenna, terahertz source.

## I. INTRODUCTION

Recently, terahertz (THz) waves have increased both researchers' interest and technological applications in security systems [1], spectroscopy [2] and medical imaging [3] to name a few. Various sources such as quantum cascade lasers (QCLs), frequency multipliers, and free-electron lasers (FELs) are utilized in THz technology, whereas each of them suffers from certain drawbacks [4]. Photoconductive antenna (PCA) is another type of THz sources which can be also used as a THz detector [5]. The PCA (also known as Auston switch [6]) converts incident optical waves into THz waves with the help of its pair of electrodes and the semiconductor material beneath them. Though working at room temperature, low cost of fabrication, and small size are the main favorable characteristics of PCAs, low

radiation power and low efficiency are their important drawbacks [7]. In order to improve these deficiencies, plasmonic PCA has been proposed by Jarrahi and co-workers [8]. In the plasmonic PCA, periodic nano-scale rods are added to each of the pair of electrodes, for the purpose of increasing optical power transmitted into the semiconductor material. Laser illumination of periodic rods of plasmonic PCA generates carriers (both holes and electrons) in the region near the rods in the semiconductor material. Concentration of carriers in the vicinity of rods causes reduction in the distance and subsequently time required for carriers to reach the electrodes. Consequently, more number of carriers can arrive at the electrodes under the acceleration induced by bias electric field. When carriers arrive at the electrodes, current is generated in the electrodes and subsequently this current is transformed into THz wave by electrodes of the plasmonic PCA.

Analysis of the performance of PCA is challenging because of the complicated interacting electromagnetic field and photonic effects in the semiconductor material. For an accurate analysis, each step of the process of optical to THz-wave conversion including laser illumination of PCA, carriers generation, carriers acceleration due to the bias voltage applied on the electrodes, and THz wave radiated by electrodes of antenna should be rigorously taken into account. In plasmonic PCA, the complexity of analysis even further increases due to the existence of nano-scale periodic rods.

In this work, a hybrid model (combining analytical formulas with finite element method) is presented in the next section for analyzing plasmonic PCAs. In section III, by the use of the proposed model, a typical plasmonic PCA is studied as an example and results of the current model are compared with measurement results of reference [9].

## II. THEORY

A plasmonic PCA as shown in Fig. 1 (a) consists of a pair of electrodes and a semiconductor material beneath them. Bias voltages are applied to the electrodes

and a laser as the source of optical wave is focused onto the semiconductor material beneath the periodic rods of anode electrode to maximize THz radiation [9]. The performance of the plasmonic PCA is mainly determined by its THz-radiated power that can be obtained by calculating the current induced on its electrodes. In plasmonic PCA, most of carriers are generated under the rods of anode electrode [9]. Moreover, here we assume that the laser illumination of rods is uniform along rods direction ( $z$ -axis of Fig. 1 (a)). Therefore, for calculating the generated current, the plasmonic PCA is assumed as a two-dimensional (2D) structure in the  $x$ - $y$  plane perpendicular to rods direction. A unit cell of periodic rods in the  $x$ - $y$  plane is shown in Fig. 1 (b); the left ( $x=0$ ) and right ( $x=d_x$ ) vertical lines are periodic boundaries and the width and height of rods are  $w_x$  and  $h_y$ , respectively. Based on plane-problem assumption, the

amount of current density,  $\mathbf{j}_c(x, y, t)$ , generated at time  $t$  and point  $(x, y)$  within the unit cell, can be calculated by ([10]):

$$\mathbf{j}_c(x, y, t) = e\mu_e n(x, y, t)\mathbf{E}_{\text{bias}}(x, y), \quad (1)$$

where  $e$  is the electron charge,  $\mu_e$  is the electron mobility in semiconductor material,  $n(x, y, t)$  is the carriers density in the semiconductor region of the unit cell as a function of position and time, and  $\mathbf{E}_{\text{bias}}(x, y)$  is the bias electric field in the semiconductor region. It should be noted that, the value of  $\mu_e$  is typically one order of magnitude larger than the value of hole mobility [11], therefore, the effect of holes in Eq. (1) is disregarded. According to Eq. (1), in order to calculate the current density,  $\mathbf{j}_c(x, y, t)$ , generated in the unit cell of plasmonic PCA, the carriers density,  $n(x, y, t)$ , and electric field,  $\mathbf{E}_{\text{bias}}(x, y)$ , should be first evaluated. The value of these quantities is calculated in the following sections separately.

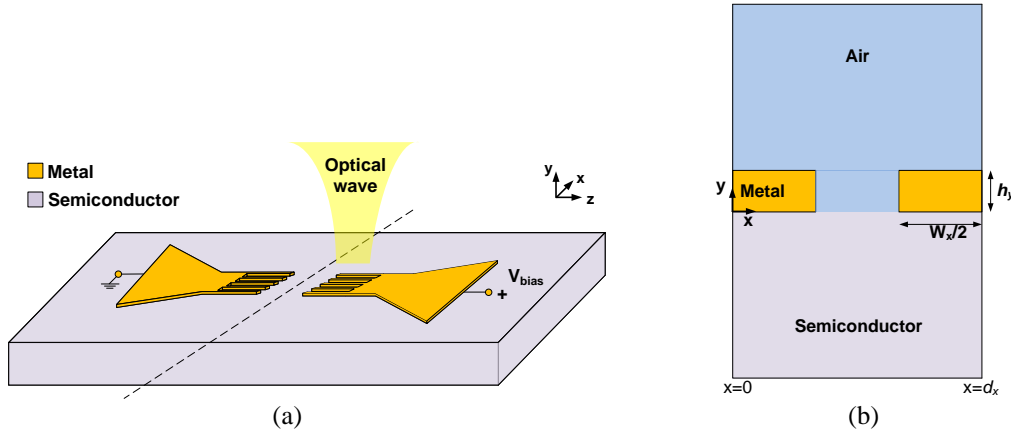


Fig. 1. (a) Schematic of a plasmonic PCA, and (b)  $x$ - $y$  plane cross section of a period of plasmonic PCA electrode. The left ( $x=0$ ) and right ( $x=d_x$ ) vertical lines are periodic boundaries.

### A. Calculation of $n(x, y, t)$

Carriers in the semiconductor region are generated due to illumination of optical wave to the rods of anode electrode. Pulses of laser power can be assumed to have a temporal Gaussian shape [10]:

$$P(t) = P_0(1 - R)e^{-2\left(\frac{t}{\tau_l}\right)^2}, \quad (2)$$

where the constant  $P_0$  is the laser peak power and  $\tau_l$  is the laser pulse duration. The dimensionless quantity  $R$  is the power reflection coefficient at the interface of air and rods of plasmonic PCA, and depends on the frequency of incident optical wave as well as permittivity constant of the semiconductor material. Since wavelength of incident optical wave is much smaller than the dimensions of each of the pair of electrodes, the value of  $R$  can be assumed independent of electrode dimensions, but depends on dimensions of rods of plasmonic PCA also. Therefore, for computing the value of  $R$ , a unit cell of 2D rods (shown in Fig. 1 (b)) are simulated by the finite element method within the COMSOL package.

Each photon of incident optical wave absorbed in the semiconductor region, generates a pair of hole and electron with capability of moving across the semiconductor material in their lifetime. In the conventional PCA with small gap between electrodes, the distribution of generated carriers (holes and electrons) can be assumed uniform in planes perpendicular to the propagation direction of incident optical power. Whereas, due to the existence of periodic rods in the electrodes of plasmonic PCA, the distribution of carriers generated in the plasmonic PCA is nonuniform, so that most of carriers are created in the vicinity of the periodic rods of the electrodes. Therefore, in order to accurately analyze the performance of plasmonic PCA, carriers density,  $n(x, y, t)$ , as a function of both time and position is required.

Temporal variation of carriers density,  $n(x, y, t)$ , depends on semiconductor material properties (which are constant values) and incident optical wave which varies with time only. On the other hand, spatial

distribution of  $n(x, y, t)$  depends on rods dimensions only. Therefore  $n(x, y, t)$  can be assumed separable in temporal- and spatial-dependencies:

$$n(x, y, t) = n_t(t)n_s(x, y), \quad (3)$$

where  $n_t(t)$  is the total carriers density (number of carriers in the unit cell in unit length of  $z$ -direction) and  $n_s(x, y)$  is the distribution of carriers density in the semiconductor region of the unit cell, normalized to unity. As will be discussed in the followings, we will obtain  $n_t(t)$  from a theoretical model, whereas  $n_s(x, y)$  is calculated by the finite element method within the COMSOL package. In practice we will calculate the electromagnetic power absorbed in semiconductor instead of  $n_s(x, y)$ , since we know that the absorbed electromagnetic power and  $n_s(x, y)$  have the same distributions down to a constant multiplier (which indeed depends on time) [12]. It is important to note that a periodic pulse (such as the incident optical wave considered herein) typically has a wide frequency band, though its power mainly concentrates at its center frequency. Therefore, to calculate the absorbed electromagnetic power (while indeed depends on the pulse frequency band), considering only the central frequency of the pulse gives results within good enough accuracy.

Let us assume that each of the two electrodes of plasmonic PCA consists of  $N$  adjacent unit cells of Fig. 1 (b) plus a pair of half cells at the farthest ends of the electrode. In the following discussion we will ignore these two half cells, inspired by the fact that their effect becomes less important as  $N$  increases. All  $N$  cells experience the same electrostatic boundary conditions as they are all subjected to one bias voltage. On the other hand, if we further assume that the incident optical wave illuminates all  $N$  cells equally, then the number of carriers  $n_t(t)$  generated in each of the  $N$  cells are the same. As the result, the total current density of plasmonic PCA,  $\mathbf{j}(x, y, t)$ , is related to the current density of each cell,  $\mathbf{j}_c(x, y, t)$ , according to:

$$\mathbf{j}(x, y, t) = N\mathbf{j}_c(x, y, t). \quad (4)$$

For calculating  $n_t(t)$ , Drude model can be used (according to the reference [12]) to write the equation:

$$\frac{dn_t(t)}{dt} = -\frac{1}{\tau_c}n_t(t) + \frac{\alpha}{hf_{opt}}\frac{P(t)}{N}, \quad (5)$$

where  $h$  is the Planck constant,  $\alpha$  is the optical absorption coefficient of semiconductor,  $\tau_c$  is carrier lifetime of semiconductor, and  $f_{opt}$  is the optical wave central frequency. In Eq. (5),  $\frac{P(t)}{N}$  is the optical power portion received by each cell. By substituting Eq. (2) into Eq. (5), and solving the resulting first-order ordinary differential equation,  $n_t(t)$  as a function of time can be obtained as:

$$n_t(t) = \frac{P_0}{N}(1-R)\frac{\sqrt{2\pi}}{4}\frac{\alpha}{hf_{opt}}\tau_l \exp\left(-\frac{1}{8}\left(\frac{\tau_l}{\tau_c}\right)^2 - \frac{t}{\tau_c}\right) \left(\operatorname{erf}\left(\sqrt{2}\frac{t}{\tau_l} - \frac{\sqrt{2}}{4}\frac{\tau_l}{\tau_c}\right) + 1\right). \quad (6)$$

After substituting Eqs. (1), (3) and (6) into Eq. (4), the expression for  $\mathbf{j}(x, y, t)$  boils down to:

$$\mathbf{j}(x, y, t) = e\mu_e P_0(1-R)\frac{\sqrt{2\pi}}{4}\frac{\alpha}{hf_{opt}}\tau_l \exp\left(-\frac{1}{8}\left(\frac{\tau_l}{\tau_c}\right)^2 - \frac{t}{\tau_c}\right) \left(\operatorname{erf}\left(\sqrt{2}\frac{t}{\tau_l} - \frac{\sqrt{2}}{4}\frac{\tau_l}{\tau_c}\right) + 1\right) n_s(x, y) \mathbf{E}_{\text{bias}}(x, y). \quad (7)$$

It is important to note that  $N$  cancels out in Eq. (7), implying that our model does not depend on the considered number of unit cells  $N$ .

## B. Calculation of $\mathbf{E}_{\text{bias}}(x, y)$

The bias voltage applied on the electrodes of plasmonic PCA, creates an electric field,  $\mathbf{E}_{\text{bias}}(x, y, z)$ , in the semiconductor region between electrodes. This field accelerates generated carriers and assists them to reach to the rods. Since most of the carriers are generated beneath the rods of anode electrode, they need to move in the plane ( $xy$ -plane of Fig. 1 (a)) perpendicular to the rods direction ( $z$ -direction of Fig. 1 (a)) to reach to the rods. Therefore, components of the electric field in this plane have the largest effect on the drift velocity of carriers in the semiconductor material. Hence, only  $x$ - and  $y$ -components of  $\mathbf{E}_{\text{bias}}(x, y, z)$ , in the semiconductor region need to be calculated. Moreover, due to the assumption that incident optical wave is focused onto the middle of rod (far from both ends) and consequently most of carriers are generated in the semiconductor region beneath the middle of rod, the effect of the both ends of rod on the bias electric field in the semiconductor region is neglected here; therefore  $\mathbf{E}_{\text{bias}}(x, y, z)$  is assumed to be invariant of  $z$  coordinate, and we will drop the  $z$  argument hereafter. In order to obtain  $\mathbf{E}_{\text{bias}}(x, y)$ , the Laplace equation  $\nabla^2 V_{\text{bias}} = 0$  ( $V_{\text{bias}}$  is the electric potential function due to the bias voltages) in companion with the Dirichlet boundary conditions of bias voltage values on the electrodes is solved in the semiconductor region of Fig. 1 (b) by COMSOL package, with  $-\nabla V_{\text{bias}} = \mathbf{E}_{\text{bias}}$ .

## C. Field screening effect

Bias electric field,  $\mathbf{E}_{\text{bias}}(x, y)$ , in the semiconductor region causes generated electrons and holes to move in opposite directions. With spatial separation between electrons and holes, polarization,  $\mathbf{p}(x, y, t)$ , is induced in the semiconductor region. The time-dependence of polarization can be calculated by solving ([12]):

$$\frac{\partial \mathbf{p}(x, y, t)}{\partial t} = -\frac{1}{\tau_r} \mathbf{p}(x, y, t) + \mathbf{j}_c(x, y, t), \quad (8)$$

where  $\tau_r$  is the recombination time of carriers. According to the point-dipole model [11], electric field induced by polarization can be expressed as:

$$\mathbf{E}_{sc}(x, y, t) = \frac{1}{\eta \epsilon} \mathbf{p}(x, y, t), \quad (9)$$

where  $\epsilon$  is the permittivity constant of semiconductor material and  $\eta$  is a coefficient which depends on the antenna structure. The direction of induced electric field,  $\mathbf{E}_{sc}(x, y, t)$ , created due to the presence of polarization, is

in opposite to the direction of bias electric field. Therefore, bias electric field is opposingly “screened” by  $\mathbf{E}_{sc}(x, y, t)$ . By taking into account the field screening effect, the generated current density of Eq. (1), should be corrected as:

$$\mathbf{j}_c(x, y, t) = e\mu_e n(x, y, t)(\mathbf{E}_{bias}(x, y) - \mathbf{E}_{sc}(x, y, t)). \quad (10)$$

Eqs. (4), (9) and (10) give:

$$\mathbf{p}(x, y, t) = \eta \varepsilon \mathbf{E}_{bias}(x, y) - \frac{\eta \varepsilon}{e\mu_e N} \frac{\mathbf{j}(x, y, t)}{n(x, y, t)}, \quad (11)$$

subsequently Eqs. (8) and (11) yield:

$$\frac{\partial \mathbf{j}(x, y, t)}{\partial t} = \frac{e\mu_e N}{\tau_r} \mathbf{E}_{bias}(x, y) n(x, y, t) + \mathbf{j}(x, y, t) \left( \frac{1}{n(x, y, t)} \frac{\partial n(x, y, t)}{\partial t} - \frac{1}{\tau_r} - \frac{e\mu_e}{\eta \varepsilon} n(x, y, t) \right). \quad (12)$$

By numerically solving Eq. (12), current density,  $\mathbf{j}(x, y, t)$ , generated in plasmonic antenna with consideration of field screening effect can be calculated.

### III. RESULTS AND DISCUSSIONS

In the previous section a hybrid model was presented for calculating current density of electrodes of plasmonic PCAs. In order to validate the accuracy of the proposed model, the current generated in electrodes of the plasmonic PCA proposed in the reference [9] is investigated herein. The plasmonic PCA of the reference [9], consists of two bow-tie electrodes placed on the low-temperature GaAs (LT-GaAs) substrate as shown in Fig. 1 (a). An optical wave from Ti:sapphire laser with a central frequency of 375 THz, repetition rate of 76 MHz, and pulse duration of 200 fs is focused onto the rods of anode electrode. Dimensions of the antenna and parameters of laser and LT-GaAs semiconductor utilized for analyzing the plasmonic PCA are given in Table 1; the values are tabulated along with their corresponding references.

Table 1: Antenna dimensions and parameters for laser and LT-GaAs semiconductor

Parameter	Value
Electron mobility for LT-GaAs [13]	$\mu_e = 0.02 \text{ m}^2\text{V}^{-1}\text{s}^{-1}$
Optical absorption coefficient [14]	$\alpha = 6000 \text{ cm}^{-1}$
Laser pulse duration [9]	$\tau_l = 200 \text{ fs}$
Laser repetition rate [9]	$f_r = 76 \text{ MHz}$
Carrier lifetime [15]	$\tau_c = 1 \text{ ps}$
Carrier recombination time [12]	$\tau_r = 100 \text{ ps}$
x-axis periodicity of rods [9]	$d_x = 200 \text{ nm}$
Width of rods [9]	$w_x = 100 \text{ nm}$
Height of rods [9]	$h_y = 50 \text{ nm}$
Permittivity constant of LT-GaAs [14]	$\varepsilon = 12.86 \varepsilon_0$
Coefficient related to the antenna structure	$\eta = 3 * 10^{-6}$
Power reflection coefficient at the interface of air and rods	$R = 0.3$

The power reflection coefficient at the interface of air and rods with rod dimensions given in Table 1 is 0.3 according to result of simulation of 2D structure (Fig. 1 (b)) within COMSOL package. For LT-GaAs semiconductor, with parameters given in Table 1, the total carriers density,  $N^*n_i(t)$ , is calculated using Eq. (6) and is plotted in Fig. 2 for different values of incident optical power  $P_0$ . From both Fig. 2 as well as Eq. (6), it can be deduced that the rise time of  $n_i(t)$  depends on the laser pulse duration,  $\tau_l$ , whereas the decay time depends on the carrier lifetime,  $\tau_c$ , of LT-GaAs.

As explained in the previous section another parameter needed for calculating generated current density,  $\mathbf{j}(x, y, t)$ , is the distribution of carriers density,  $n_s(x, y)$ . In order to compute  $n_s(x, y)$ , 2D rods (shown in Fig. 1 (b)) with parameters of Table 1 are simulated within the COMSOL package. Obtained values for the distribution of carriers density,  $n_s(x, y)$ , are shown in Fig. 3. As it can be seen in this figure, most of carriers are generated in the vicinity of rods especially near the corners; such that, the distance of most of generated carries to the nearest rod is less than 40 nm. Next the values obtained for  $n_s(x, y)$  and  $n_i(t)$  are used in Eq. (3) to result in the carriers density,  $n(x, y, t)$ .

As mentioned earlier also, electric field,  $\mathbf{E}_{bias}(x, y)$ , in the semiconductor region, created by bias voltage, should be first determined for calculating generated current density  $\mathbf{j}(x, y, t)$  in the electrodes of the plasmonic PCA. Therefore, within the COMSOL package, the Laplace equation is solved numerically in the LT-GaAs semiconductor region. Dirichlet boundary conditions for the Laplace equation are the bias voltage values at anode and cathode electrodes, set as 40 V and 0 V, respectively [9]. The absolute value of the bias electric field,  $\mathbf{E}_{bias}(x, y)$ , in the semiconductor region beneath a period of rods determined from the simulation is shown in Fig. 4. It shows that the magnitude of  $\mathbf{E}_{bias}$  drastically decreases with the increase of the distance from the rods of electrodes along the y-axis.

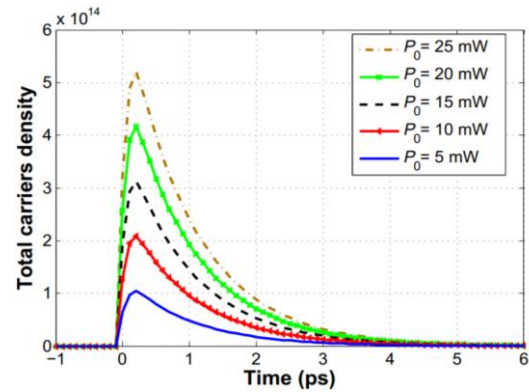


Fig. 2. Total carriers density,  $N^*n_i(t)$ , in the LT-GaAs semiconductor of the plasmonic PCA versus time for different values of optical power,  $P_0$ .

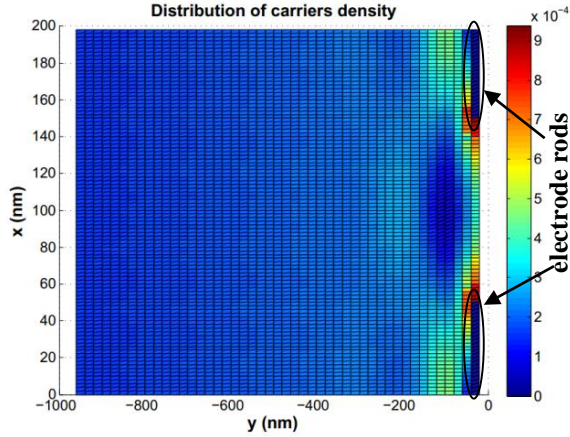


Fig. 3. The distribution of carriers density,  $n_s(x,y)$ , in LT-GaAs semiconductor beneath a period of rods of plasmonic PCA electrode.

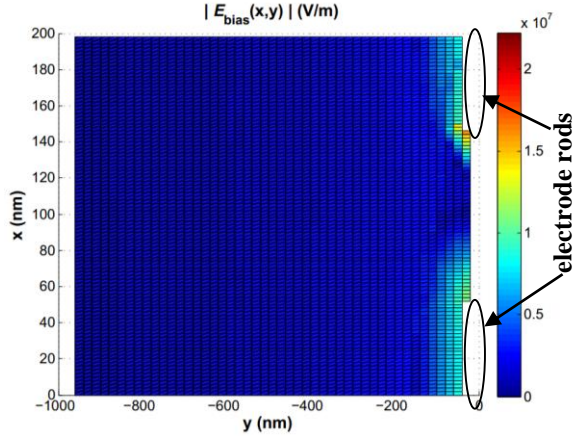


Fig. 4. The magnitude of bias electric field in the semiconductor region of a period of the plasmonic PCA electrode obtained from simulation.

Using the calculated carriers density,  $n(x,y,t)$ , and bias electric field,  $E_{\text{bias}}(x,y)$ , the current density,  $j(x,y,t)$ , generated in the plasmonic PCA is finally determined from both Eq. (12) with field screening effect and Eq. (4) without field screening effect. The generated currents (averaged over time) are calculated by the proposed model and are shown in Fig. 5 as a function of incident optical power. Along with them, measurement results of [9] are also plotted. It can be observed that in comparison with the measurement results, the theoretical results obtained by Eq. (12) with considering field screening effect (red solid curve of Fig. 5) are more accurate than the theoretical results obtained by Eq. (4) without considering field screening effect (green dashed curve of Fig. 5). To the best of the author's knowledge, this is the most accurate theoretical results for plasmonic PCA mimicking experimental observations, reported as far in

the literature.

The difference between red solid curve and green dashed curve of Fig. 5 corresponds to the reduction of current generated in the plasmonic PCA due to the field screening effect. At low incident optical power, the field screening effect is negligible, however, this effect amplifies with the increase of optical power. As the number of generated carriers increases due to the increase of optical power, the polarization induced by spatial separation of them also increases; and consequently the field screening effect intensifies. On the other hand, according to Eq. (10) the increase of field screening effect leads to reduction in the rate of current generated in plasmonic PCA as can be also observed in Fig. 5; this is also consistent with the measurement results of reference [9].

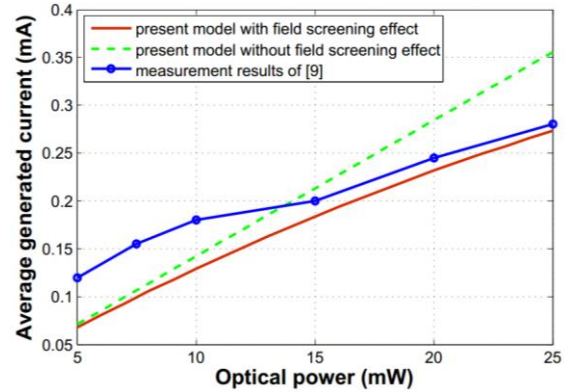


Fig. 5. Average current generated in the plasmonic PCA with the parameters given in Table 1.

#### IV. CONCLUSION

Plasmonic photoconductive antennas (plasmonic PCAs) have broad technological applications as terahertz (THz) sources. On the theoretical side, however, the analysis of these antennas (PCAs) is very challenging due to the existence of periodic structures. In this paper, a hybrid model consisting of both analytical and numerical methods was proposed which significantly reduces the complexity of plasmonic PCA analysis and subsequently the time required for its simulation. The model ultimately calculates the current generated in the electrodes of plasmonic PCA. For this purpose, the time-dependence and spatial-dependence of density of carriers generated in the semiconductor of plasmonic PCA were studied separately; the time-dependence was calculated analytically, whereas the spatial-dependence was computed using finite element method. For validation purpose, a typical plasmonic PCA as an example was analyzed by the model, and was found that model results match very well with experimental measurements published earlier in the literature. It was shown that field screening effect in the plasmonic PCA is negligible at

low incident optical power. However, this effect gets substantial as the optical power increases. The increase of field screening effect causes the rate of current generated in the plasmonic PCA to reduce. This fact can also be confirmed from the measurement results of plasmonic PCAs reported earlier.

## REFERENCES

- [1] N. Karpowicz, H. Zhong, C. Zhang, K. I. Lin, J. S. Hwang, J. Xu, and X. C. Zhang, "Compact continuous-wave subterahertz system for inspection applications," *Appl. Phys. Lett.*, 86, 054105, 2005.
- [2] E. Pickwell and V. P. Wallace, "Biomedical applications of terahertz technology," *J. Phys. D: Appl. Phys.*, vol. 39, pp. R301-R310, 2006.
- [3] H. Hoshina, A. Hayashi, N. Miyoshi, F. Miyamaru, and C. Otani, "Terahertz pulsed imaging of frozen biological tissues," *Appl. Phys. Lett.*, 94, 123901, 2009.
- [4] X. Yin, B. Ng, and D. Abbott, *Terahertz Imaging for Biomedical Applications: Pattern Recognition and Tomographic Reconstruction*. © Springer Science Business Media LLC, 2012.
- [5] N. Wang, M. R. Hashemi, and M. Jarrahi, "Plasmonic photoconductive detectors for enhanced terahertz detection sensitivity," *Optics Express*, vol. 21, no. 14, pp. 17221-17227, 2013.
- [6] D. H. Auston, "Picosecond optoelectronic switching and gating in silicon," *Appl. Phys. Lett.*, vol. 26, pp. 101-103, 1975.
- [7] D. S. Kim and D. S. Citrin, "Coulomb and radiation screening in photoconductive terahertz sources," *App. Phys. Lett.*, 88, 161117 365, 2006.
- [8] C. Berry and M. Jarrahi, "High-performance photoconductive terahertz sources based on nanoscale contact electrode gratings," *IEEE Int. Microwave Symp. Digest (MTT)*, Montreal, Canada, 17-22 June 2012.
- [9] C. W. Berry, M. R. Hashemi, M. Unlu, and M. Jarrahi, "Significant radiation enhancement in photoconductive terahertz emitters by incorporating plasmonic contact electrodes," *Nature Communications*, 4, Article number: 1622, doi: 10.1038/ncomms2638, 2013.
- [10] N. Khiabani, Y. Huang, Y. Shen, and S. Boyes, "Theoretical modeling of a photoconductive antenna in a terahertz pulsed system," *IEEE Trans. on Antennas and Propagat.*, 61, no. 4, 1538, 2013.
- [11] G. C. Loata, *Investigation of low-temperature-grown GaAs photoconductive antenna for continuous-wave and pulsed terahertz generation*, (Ph.D. dissertation), Goethe-University, Frankfurt, 2007.
- [12] P. U. Jepsen, R. H. Jacobsen, and S. R. Keiding, "Generation and detection of terahertz pulses from biased semiconductor antennas," *J. Opt. Soc. Am. B*, vol. 13, no. 11, 1996.
- [13] M. Tani, S. Matsuura, K. Sakai, and S. Nakashima, "Emission characteristics of photoconductive antennas based on low-temperature-grown GaAs and semi-insulating GaAs," *Appl. Opt.*, vol. 36, no. 30, pp. 7853-7859, 1997.
- [14] J. Piprek, *Semiconductor Optoelectronic Devices Introduction to Physics and Simulation*, Academic Press an imprint of Elsevier Science, ISBN:0-12-557190-9, p. 230, 2003.
- [15] M. C. Beard, G. M. Turner, and C. A. Schmuttenmaer, "Subpicosecond carrier dynamics in low-temperature grown GaAs as measured by timeresolved terahertz spectroscopy," *J. Appl. Phys.*, vol. 90, no. 12, pp.5915-5923, 2001.



**Mohammadreza Khorshidi** was born in Birjand, Iran in 1983. He received the Master of Science (M.Sc.) degree in 2009 from K.N. Toosi University of Technology, Iran. He is now Ph.D. candidate in Communication Engineering in Shahed University. His main research interest is terahertz technology, with focus on photoconductive antennas and plasmonic structures.



**Gholamreza Dadashzadeh** was born in Urmia, Iran, in 1964. He received Ph.D. degrees in Communication Engineering from Tarbiat Modarres University, Tehran, Iran. He is currently an Associate Professor with the Department of Electrical Engineering, Shahed University, Tehran. He has published more than 70 papers in referred journals and international conferences in the area of antenna design and smart antennas.